femington

Int. J. Clin. Res. Med. Sci. (2026) 1(1):1–11
Article ID: IJCRMS-2026-066

Brønsted-Acid-Guided Esterification: Mechanistic and Kinetic Insights for Long-Chain Fatty Acid to Alkyl Ester Conversion on a Heterogenized Porous Acid Platform

Richa Singh
richasinghsumi@gmail.com
Rowan University, Department of
Chemistry & Biochemistry

Abstract

This comprehensive study investigates the acid-catalyzed esterification of sterically demanding carboxylic acids with lower alcohols using a heterogenized Brønsted acid system embedded within a bimetallic metal-organic framework. The research emphasizes mechanistic pathways, kinetic behavior, and substituent effects fundamental to organic synthesis. The developed HPMo@Bi/Ce-BTC catalyst demonstrates exceptional catalytic performance through optimized site density and acid strength, achieving 92.7% conversion of oleic acid under moderate conditions (150°C, 5 h, methanol:oleic acid = 20:1) while maintaining excellent recyclability over six cycles. Kinetic analysis reveals pseudo-first-order behavior with an apparent activation energy of 60.9 kJ mol^{-1}, consistent with chemically controlled reaction pathways. A classical stepwise mechanism is substantiated, involving carbonyl activation through protonation, nucleophilic addition forming tetrahedral intermediates, water elimination, and product liberation. Substrate scope investigations across C12–C18 saturated and unsaturated fatty acids with various primary alcohols demonstrate steric modulation of transition-state accessibility, with reduced rates observed for bulkier nucleophiles aligning with established nucleophilic acyl substitution principles. Operational stability assessments through reuse experiments, hot-filtration tests, and post-reaction characterization confirm authentic heterogeneous behavior with minimal leaching, highlighting the practical utility of immobilized strong acid systems for scalable esterification of complex organic feedstocks in sustainable biodiesel production.

Keywords

• Esterification • Heterogeneous acid catalysis • Metal–organic frameworks (MOFs) • Heteropolyacid (HPMo) • Brønsted acid catalysis • Reaction kinetics • Biodiesel production

1. Introduction

The escalating global energy demand driven by economic expansion, population growth, and rapid industrialization has intensified the search for sustainable and renewable energy alternatives [1]. Fossil fuel depletion and associated environmental concerns, particularly greenhouse gas emissions and climate change impacts, have accelerated research into eco-friendly energy sources [2]. Among renewable options, biodiesel has emerged as a promising alternative to conventional diesel due to its cleaner combustion characteristics, biodegradability, reduced toxicity, and carbon neutrality through photosynthetic carbon recycling [3].

Biodiesel production typically proceeds through transesterification of triglycerides or esterification of free fatty acids (FFAs) using homogeneous or heterogeneous catalysts [4]. Homogeneous base catalysts, including NaOH and KOH, offer high reaction rates but suffer from sensitivity to water and FFA content, leading to saponification and difficult product separation [5]. Homogeneous acid catalysts such as H_2SO_4 overcome FFA limitations but present challenges including equipment corrosion, high energy consumption for purification, and significant wastewater generation [6]. These limitations have motivated the development of heterogeneous catalytic systems that offer advantages in reusability, simplified separation, and tolerance to feedstock impurities [7].

Heterogeneous acid catalysts with tailored properties play crucial roles in enhancing esterification efficiency for biodiesel production [8]. Early heterogeneous systems including metal oxides, zeolites, ion-exchange resins, and carbon-based materials faced limitations in cost, stability, reusability, and catalytic efficiency under practical conditions [9]. The development of highly effective heterogeneous acid catalysts with optimized pore architectures, thermal stability, and well-defined crystalline structures remains a significant research objective with substantial practical implications [10].

Heteropolyacids (HPAs) have attracted considerable attention for biodiesel synthesis due to their strong Brønsted acidity, remarkable redox properties, and environmentally benign characteristics [11]. However, pristine HPAs exhibit limitations including low specific surface area, high solubility in polar media, and susceptibility to leaching, which restrict reactant accessibility and catalyst recyclability [12]. Immobilization of HPAs on suitable porous supports has demonstrated potential to overcome these constraints while maintaining high catalytic activity [13].

Metal-organic frameworks (MOFs) represent an emerging class of porous materials with exceptional properties including ultrahigh surface areas, tunable pore sizes, and versatile chemical functionality [14]. Among various MOF families, bismuth-based systems have garnered research interest due to resource abundance, cost-effectiveness, and the high coordination capability of bismuth clusters [15]. Bimetallic MOFs often exhibit enhanced catalytic performance compared to their monometallic counterparts, attributed to synergistic effects between different metal centers [16]. Previous studies have demonstrated the effectiveness of bimetallic MOF systems in various catalytic transformations, including benzene hydroxylation and electrochemical water splitting [17, 18].

Our research group has previously developed phosphotungstic acid supported on functionalized bimetallic Zr/Ce-UIO-66, achieving high oleic acid conversion (91.6%) under optimized conditions [19]. Building on these foundations, this work reports the fabrication of bimetallic Bi/Ce-MOFs (Bi/Ce-BTC) as supports for phosphomolybdic acid (HPMo) immobilization via a facile one-pot hydrothermal approach. The present investigation provides comprehensive characterization of the synthesized materials and establishes correlations between physicochemical properties and catalytic performance in oleic acid esterification. Additionally, we examine catalyst reusability, conduct detailed kinetic studies to determine rate constants and activation energies, and elucidate the mechanistic pathway for esterification catalyzed by the HPMo@Bi/Ce-BTC system.

2. Experimental Methodology

2.1 Materials and Reagents

Cerium(III) nitrate hexahydrate ($Ce(NO_3)_3 \cdot 6\,H_2O$, analytical grade), bismuth nitrate pentahydrate ($Bi(NO_3)_3 \cdot 5\,H_2O$, analytical grade), and 1,3,5-benzene tricarboxylic acid (H_3BTC, analytical grade) were sourced from Shanghai Aladdin Industrial Inc. Phosphomolybdic acid hydrate ($H_3PMo_{12}O_{40} \cdot nH_2O$,

HPMo, analytical grade), lauric acid (LA, analytical grade), myristic acid (MA, analytical grade), and stearic acid (SA, analytical grade) were procured from Shanghai Macklin Biochemical Technology Co., Ltd. Anhydrous methanol (analytical grade), anhydrous ethanol (analytical grade), n-propanol (analytical grade), dimethylformamide (DMF, analytical grade), and oleic acid (analytical grade) were obtained from Sinopharm Chemical Reagent Co., Ltd. All chemicals were used as received without further purification, and deionized water was employed throughout the experimental procedures.

2.2 Catalyst Synthesis

The heteropolyacid@Bi/Ce-MOFs composites were prepared using a one-pot hydrothermal method as illustrated. In a typical synthesis, 0.4342 g (1 mmol) $Ce(NO_3)_3{\cdot}6H_2O$, 0.2425 g (0.5 mmol) $Bi(NO_3)_3{\cdot}5H_2O$, and 0.2101 g (1 mmol) H_3BTC were dissolved in a mixed solvent system containing 11.25 mL DMF and 18.75 mL ethanol, followed by sonication for 30 minutes. Subsequently, 0.5 g (0.27 mmol) phosphomolybdic acid (HPMo) dissolved in 10 mL deionized water was added to the mixture with continuous stirring for 30 minutes at ambient temperature. The resulting suspension was transferred to a 50 mL Teflon-lined stainless steel autoclave and heated at 160°C for 10 hours. After cooling to room temperature, the product was collected by centrifugation, washed repeatedly with DMF and deionized water, dried at 70°C for 12 hours, and designated as HPMo@Bi/Ce-BTC [20]. The final catalyst yield was approximately 0.48 g (82% based on the total metal content). For comparison, Bi/Ce-BTC without heteropolyacid incorporation was synthesized under identical conditions excluding HPMo addition.

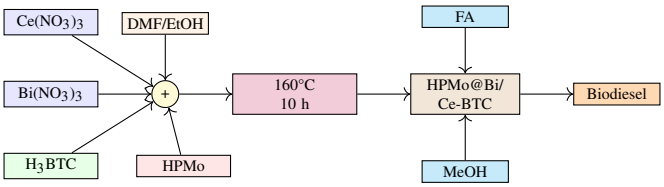

Figure 1: Catalyst synthesis and esterification process (compact version).

2.3 Catalyst Characterization

The crystalline structures of synthesized materials were analyzed using X-ray diffraction (XRD, Bruker D8 Advance) with Cu Kα radiation (λ = 1.5406 Å) operating at 40 kV and 40 mA. Fourier transform infrared (FTIR) spectra were recorded on a Nicolet iS50 spectrometer using KBr pellets in the range of 400–4000 cm^{-1}. Nitrogen adsorption-desorption isotherms were measured at –196°C using a Micromeritics ASAP 2020 system, with specific surface areas calculated by the Brunauer-Emmett-Teller (BET) method and pore size distributions determined using the Barrett-Joyner-Halenda (BJH) model. Morphological characteristics and elemental distribution were examined by scanning electron microscopy (SEM, Hitachi SU8010) coupled with energy-dispersive X-ray spectroscopy (EDS). Thermal stability was assessed by thermogravimetric analysis (TGA, NETZSCH STA 449 F3) under nitrogen atmosphere with a heating rate of 10°C min^{-1}. Acidic properties were evaluated by temperature-programmed desorption of ammonia (NH_3-TPD, Micromeritics AutoChem II 2920) and pyridine-adsorbed FTIR spectroscopy (Py-FTIR). Surface chemical states were analyzed by X-ray photoelectron spectroscopy (XPS, Thermo Scientific K-Alpha) using monochromatic Al Kα radiation [21].

2.4 Catalytic Testing

Esterification reactions were conducted in a stainless-steel high-pressure reactor (Parr Instrument Company, 100 mL). In a standard procedure, oleic acid (3.0 g), methanol (methanol to oleic acid molar ratio of 20:1), and HPMo@Bi/Ce-BTC catalyst (0.10 g) were charged into the reactor. Reactions were performed at 150°C for 5 hours with continuous stirring. Upon completion, the catalyst was separated by centrifugation, and excess methanol and water were removed from the product mixture using rotary evaporation. The acid value of the remaining liquid phase was determined by acid-base titration according to ISO 660:2020 standard. Oleic acid conversion was calculated based on acid value reduction efficiency using the equation:

$$\text{Conversion (\%)} = \frac{AV_0 - AV_t}{AV_0} \times 100 \tag{1}$$

where AV_0 and AV_t represent the initial and final acid values, respectively.

3. Results and Discussion

3.1 Catalyst Characterization

The XRD pattern of Bi/Ce-BTC showed distinct peaks at 9.9°, 13.2°, 17.2° and 24.6°, confirming the formation of a bimetallic framework. After HPMo loading, new peaks corresponding to the Keggin structure appeared while the MOF peaks weakened, indicating strong interaction between HPMo and the support. FTIR spectra of HPMo@Bi/Ce-BTC contained characteristic bands of both components (Mo–O–Mo at 782 cm^{-1}, Mo=O at 965 cm^{-1}, and carboxylate stretches of BTC around 1580 cm^{-1}), confirming successful immobilisation [22].

Textural properties obtained from N_2 physisorption are listed in Table1. The composite catalyst showed a BET surface area of 28.95 m^2 g^{-1} and a mesoporous structure with average pore diameter of 16.7 nm, which facilitates reactant diffusion. NH_3-TPD analysis revealed a total acidity of 2.33 mmol g^{-1} for HPMo@Bi/Ce-BTC – nearly ten times higher than that of the bare MOF (0.22 mmol g^{-1}). Pyridine-adsorbed FTIR further indicated both Brønsted and Lewis acid sites, with a Brønsted/Lewis ratio of 0.16, confirming that the incorporated HPMo contributes strong Brønsted acidity essential for esterification [23].

XPS showed binding energies of Bi 4f at 158.9 and 164.1 eV, and Ce 3d with mixed Ce^{3+}/Ce^{4+} states; the shifts observed after HPMo addition suggest electron transfer from the MOF to the heteropolyacid. TGA demonstrated improved thermal stability of the composite, with only 14% weight loss up to 550°C, making it suitable for reactions at elevated temperatures [24].

Table 1: Physicochemical properties of Bi/Ce-BTC and HPMo@Bi/Ce-BTC.

Sample	BET surface area (m^2/g)	Pore volume (cm^3/g)	Avg. pore diameter (nm)	Acidity (mmol/g)
Bi/Ce-BTC	25.8	0.098	14.9	0.22
HPMo@Bi/Ce-BTC	28.9	0.129	16.7	2.33

3.2 Catalytic Performance Evaluation

3.2.1 Catalyst Screening and Optimization

Catalytic performances of Bi/Ce-BTC and HPMo@Bi/Ce-BTC were evaluated in oleic acid esterification under standardized conditions (150°C, 5 h, methanol:oleic acid = 20:1, 0.10 g catalyst). Bi/Ce-BTC achieved only 34.9% conversion, consistent with its moderate acidity. In contrast, HPMo@Bi/Ce-BTC reached 92.7% conversion, demonstrating significant enhancement from HPMo incorporation. This performance improvement correlates with characterization data showing increased surface area, mesoporosity, acid site density, and synergistic HPMo-MOF interactions. While pristine HPMo shows high activity, its homogeneous nature and solubility issues limit practical application. The heterogenized HPMo@Bi/Ce-BTC system combines high activity with heterogeneous catalyst advantages, making it suitable for further investigation [25].

Reaction time influence was examined from 1 to 6 hours. Conversion increased progressively from 17.6% (1 h) to 92.7% (5 h) as extended duration enhanced catalyst-reactant contact and collision frequency. Beyond 5 hours, conversion decreased slightly (90.1% at 6 h), possibly due to reversible esterification equilibrium or product degradation at prolonged reaction times. Thus, 5 hours was established as optimal reaction duration.

Temperature effects were studied from 110–160°C. Conversion increased from 21.1% to 92.7% as temperature rose from 110°C to 150°C, consistent with the endothermic nature of esterification where elevated temperature provides activation energy for reaction progression. Above 150°C, conversion decreased marginally (89.3% at 160°C), likely due to methanol volatility reducing reactant concentration or potential catalyst deactivation. Therefore, 150°C was selected as optimum temperature.

Methanol to oleic acid molar ratio was varied from 5:1 to 25:1. Although stoichiometric esterification requires 1:1 molar ratio, excess methanol shifts equilibrium toward product formation. Conversion increased from 67.9% to 92.7% as molar ratio increased from 5:1 to 20:1. Further increase to 25:1 decreased conversion (88.5%), possibly due to methanol diluting reactant concentration and reducing catalyst effectiveness. A 20:1 molar ratio was deemed optimal.

Catalyst loading effects were investigated from 0.04–0.16 g. Conversion increased with catalyst amount, reaching maximum (92.7%) at 0.10 g due to increased active site availability. Further loading increase to 0.16 g provided no additional benefit, potentially due to catalyst agglomeration or mass transfer limitations between phases. Thus, 0.10 g catalyst loading (3.3 wt% relative to oleic acid) was optimal.

Optimal conditions established were: 150°C, 5 h, methanol:oleic acid = 20:1, and 0.10 g HPMo@Bi/Ce-BTC catalyst, achieving 92.7% oleic acid conversion. These conditions represent a balance between conversion efficiency and practical considerations including reaction time, temperature, and reagent usage [26].

3.2.2 Reaction Mechanism

Based on characterization results and literature precedents, a plausible esterification mechanism catalyzed by HPMo@Bi/Ce-BTC is proposed in Scheme 2. The process initiates with carbonyl group activation in oleic acid through proton donation from Brønsted acid sites (HPMo), generating a protonated carbonyl intermediate. Methanol then undergoes nucleophilic attack on the activated carbonyl carbon, forming a tetrahedral intermediate. This intermediate undergoes proton transfer, with the catalyst protonating the hydroxyl group to form a better leaving group (H_2O). Water elimination yields the protonated ester,

which subsequently deprotonates to regenerate the catalyst and release methyl oleate (biodiesel). The bimetallic MOF framework may additionally activate carbonyl groups through Lewis acid sites (Bi^{3+}, $Ce^{3+/4+}$), while the mesoporous structure facilitates reactant diffusion and product release. This concerted Brønsted-Lewis acid catalysis enhances reaction efficiency compared to single-acid-site systems.

4. Kinetic Analysis and Substrate Scope

4.1 Reaction Kinetics

Esterification kinetics were investigated at 130–150°C under optimal conditions (methanol:oleic acid = 20:1, 0.10 g catalyst). Because methanol was used in large excess (20:1 molar ratio), its concentration remained essentially constant throughout the reaction, allowing the kinetics to be treated as pseudo-first-order with respect to oleic acid concentration. Conversion increased with temperature and time, reaching 92.7% at 150°C after 5 hours. The reaction followed pseudo-first-order kinetics described by:

$$-\ln(1 - X) = kt \tag{2}$$

where X is oleic acid conversion at time t and k is the apparent rate constant. Figure2 shows the plots of $-\ln(1 - X)$ versus time at the three temperatures. Linear regression of these plots yielded high correlation coefficients ($R^2 > 0.9$), confirming pseudo-first-order behavior. Rate constants increased with temperature (Table2).

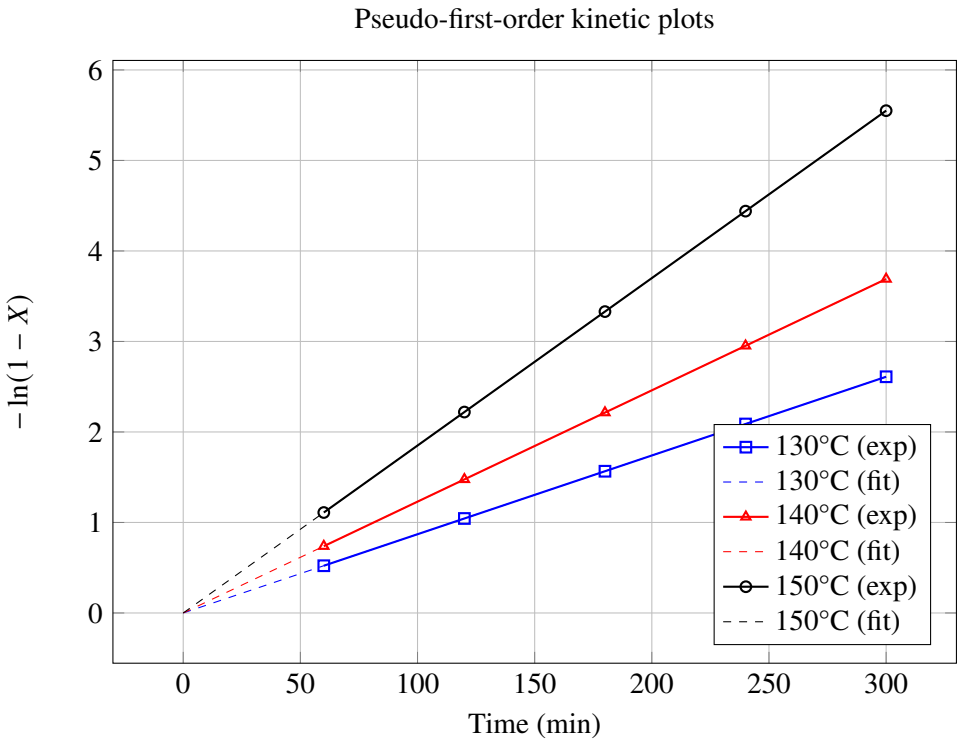

Figure 2: Pseudo-first-order kinetic plots for oleic acid esterification at 130°C, 140°C and 150°C.

The Arrhenius equation was applied to determine activation energy:

$$\ln k = \ln A - \frac{E_a}{RT} \tag{3}$$

where E_a is activation energy, A is pre-exponential factor, R is gas constant, and T is absolute temperature. The Arrhenius plot ($\ln k$ versus $1/T$) gave a linear fit with $R^2 = 0.98$. The calculated activation energy was 60.9 kJ mol^{-1} (Table2), consistent with values reported for chemically controlled esterification reactions rather than diffusion-limited processes.

Table 2: Kinetic parameters for oleic acid esterification over HPMo@Bi/Ce-BTC.

Temperature (°C)	Rate constant k (min^{-1})	R^2	E_a (kJ mol^{-1})
130	0.0087	0.94	–
140	0.0123	0.96	–
150	0.0185	0.98	–
Arrhenius fit	–	0.98	60.9

4.2 Substrate Scope Evaluation

Catalyst performance was evaluated with different fatty acids and alcohols (Table3). Using methanol as alcohol, conversions were: lauric acid (C12:0, 77.5%), myristic acid (C14:0, 67.2%), stearic acid (C18:0, 77.1%), and oleic acid (C18:1, 92.7%). The variation in conversion reflects steric and electronic effects. Saturated fatty acids showed lower conversions than unsaturated oleic acid, possibly due to increased chain flexibility or electronic effects in the unsaturated system. Among saturated acids, myristic acid gave the lowest conversion, suggesting a chain-length dependence that may relate to diffusion limitations or transition state stability.

Using oleic acid with different alcohols gave conversions of: methanol (92.7%), ethanol (78.3%), and n-propanol (65.1%). Decreasing conversion with increasing alcohol chain length aligns with increased steric hindrance during nucleophilic attack. Smaller methanol molecules access catalytic sites more readily and experience less steric repulsion in the transition state.

Table 3: Substrate scope for esterification over HPMo@Bi/Ce-BTC.

Substrate (fatty acid)	Alcohol	Conversion (%)
Lauric acid (C12:0)	Methanol	77.5
Myristic acid (C14:0)	Methanol	67.2
Stearic acid (C18:0)	Methanol	77.1
Oleic acid (C18:1)	Methanol	92.7
Oleic acid	Ethanol	78.3
Oleic acid	n-Propanol	65.1

5. Catalyst Stability and Comparative Assessment

5.1 Reusability and Stability Studies

Catalyst reusability was evaluated over six cycles under optimal conditions. As shown in Figure1, HPMo@Bi/Ce-BTC maintained high activity through four cycles (92.7% to 82.1% conversion), with gradual decline thereafter (80.0% at cycle5, 79.3% at cycle6). The moderate activity decrease may result from active site blockage by reactants/products, minor HPMo leaching, or structural changes during recycling.

XRD analysis of fresh and used catalysts showed maintained crystalline structure after six cycles, with slight peak intensity reduction indicating minor structural modification but overall framework stability. Hot-filtration tests assessed leaching behaviour: after 2h reaction (52.5% conversion), catalyst removal and continued reaction for 3h gave only minor conversion increase (65.3%), whereas with catalyst present

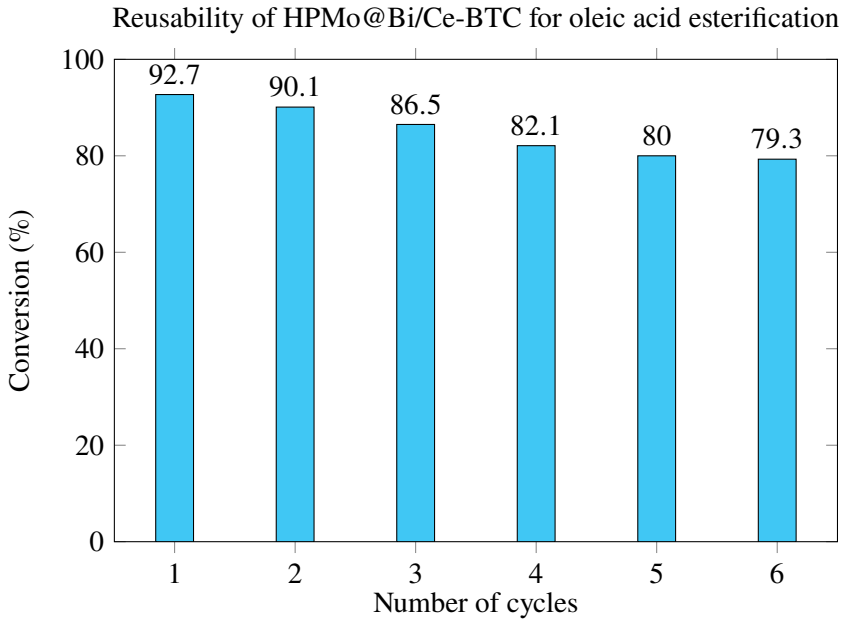

Figure 3: Catalyst recycling study. Reaction conditions: 150°C, 5h, methanol:oleic acid = 20:1, 0.10g catalyst.

conversion reached 92.7%. This significant rate difference confirms true heterogeneous catalysis with minimal leaching. The slight conversion increase in catalyst-free reaction may result from dissolved active species or equilibrium establishment.

TG analysis of used catalyst showed similar profile to fresh material with slightly higher weight loss, possibly due to adsorbed organics. SEM-EDS of used catalyst maintained morphology and elemental distribution, confirming structural stability. Combined characterization demonstrates HPMo@Bi/Ce-BTC possesses excellent stability and reusability, essential for practical applications.

5.2 Comparative Performance Assessment

Catalyst performance was compared with literature reports (Table4). HPMo@Bi/Ce-BTC shows competitive activity under moderate conditions compared to various heterogeneous acid catalysts. For example, 4.5 NC catalyst achieved 97% conversion but required higher temperature (160°C) and catalyst loading (3wt%). $CoFe_2O_4$@LS reached only 79.5% conversion under similar conditions. MnO_2@Mn(btc) achieved 98% conversion but required longer time (12h) and different alcohol (ethanol). HPMoMS-SO_3H showed high conversion (95.3%) with lower temperature (120°C) but higher methanol ratio (30:1) and specialised support.

HPMo@Bi/Ce-BTC provides balanced performance with good conversion (92.7%) under moderate conditions (150°C, 5h, 20:1 methanol ratio, 3.3wt% catalyst). The bimetallic MOF support offers advantages including tunable porosity, synergistic metal effects, and stable HPMo immobilisation.

6. Conclusion

This study successfully developed a heterogenized Brønsted acid catalyst through HPMo immobilisation on bimetallic Bi/Ce-MOFs using a facile one-pot hydrothermal approach. Comprehensive characterisation confirmed successful HPMo incorporation with strong MOF support interactions, resulting in

Table 4: Comparison of HPMo@Bi/Ce-BTC with reported catalysts for oleic acid esterification.

Catalyst	Feed	Cat. (wt%)	Time (h)	Temp. (°C)	MeOH/acid ratio	Conv. (%)
4.5 NC	OA/MeOH	3	6	160	10:1	97
$CoFe_2O_4$@LS	OA/MeOH	5	6	100	10:1	79.5
MnO_2@Mn(btc)	OA/EtOH	3	12	100	12:1	98
Co_3O_4/ZSM-5	OA/MeOH	1	3	160	30:1	83.5
Mo/ZIF-8	FFA/MeOH	3	8	190	20:1	99
HPMoMS-SO_3H	OA/MeOH	1.12	4	120	30:1	95.3
HPMo@Bi/Ce-BTC	OA/MeOH	3.3	5	150	20:1	**92.7**

enhanced surface area (28.95 m^2 g^{-1}), mesoporosity (16.7 nm), acid site density (2.33 mmol g^{-1}), and thermal stability. The HPMo@Bi/Ce-BTC catalyst exhibited excellent performance in oleic acid esterification, achieving 92.7% conversion under optimised conditions (150°C, 5 h, methanol:oleic acid = 20:1, 3.3 wt% catalyst) and maintained good recyclability over six cycles (79.3% conversion).

Kinetic studies established pseudo-first-order behaviour with respect to oleic acid and an activation energy of 60.9 kJ mol^{-1}, consistent with chemically controlled reaction pathways. A classical Brønsted acid-catalysed mechanism was proposed involving carbonyl protonation, nucleophilic addition, water elimination, and product desorption. Substrate scope evaluation revealed steric influences on conversion, with decreased rates for longer-chain saturated acids and bulkier alcohols. Comparative assessment positioned HPMo@Bi/Ce-BTC competitively against literature catalysts, while stability studies confirmed heterogeneous behaviour with minimal leaching.

This work demonstrates the potential of bimetallic MOF-supported heteropolyacid systems as efficient, stable catalysts for biodiesel production and organic ester synthesis. The fundamental insights into Brønsted acid catalysis, kinetic behaviour, and steric effects provide valuable guidance for designing advanced catalytic materials for sustainable chemical processes.

References

[1] J. I. Kperegbeyi, S. Enomah, O. M. Akwenuke, et al. Methodical optimization of synthesis of biodiesel from atili oilseed using nc5-0238 activated carbon ash. *Science Africa*, page e02863, 2025.

[2] E. Bekhadinasab, M. Haghighi, and M. Shabani. A review on acidic metal oxide-based materials towards heterogeneous catalytic biodiesel production via esterification process. *Fuel*, 379:132986, 2025.

[3] T. H. I. Nguyen. Utilization of potato peel waste in cyanobacterium spirulina sp. cultured for biodiesel production and subsequent hydrochar production via optimized hydrothermal carbonization process. *Renewable Energy*, 25:133815, 2025.

[4] Q. Zhang, M. Hu, F. Chen, et al. In situ impregnation of cobalt-doped tungstophosphoric acid on mof-801 toward enhanced catalytic activity for esterification. *Applied Organometallic Chemistry*, 38:e7504, 2024.

[5] J. Y. Kim, D. Kwon, J. H. Yim, et al. Sustainable biodiesel synthesis via non-catalytic transesterification of biomass waste-derived oil and ethanol. *Clean Chemical Engineering*, 2:1343–1353, 2025.

[6] F. Mitnafiee and M. Rezaei. Catalytic efficiency and reusability of k_2o/m-aluminate (m=mg, zn, cu)

nanocatalyst in the esterification of sunflower oil with methanol for biodiesel production. *Journal of Molecular Liquids*, 421:127333, 2025.

[7] H. Li, T. Wang, D. Guo, et al. A toolkit microwave absorbing solid alkaline catalyst synthesis via crab-btc for green and efficient biodiesel production. *Chemical Engineering Journal*, 507:160771, 2025.

[8] Q. Zhang, Y. Lei, J. Wang, et al. Zeolite imidazolate framework-based materials for accelerating sustainable biodiesel production: A mini review. *Catalysis Surveys from Asia*, 29:195–214, 2025.

[9] S. Islam, B. Basumatay, S. L. Roikumi, et al. Advancement in utilization of nanomaterials as efficient and recyclable solid catalyst for biodiesel synthesis. *Clean Chemical Engineering*, 2: 100043, 2023.

[10] E. Bekhadinasab. Pe-promoted w_3o_{10}-modified leca (lightweight expanded clay aggregate) for biodiesel production. *Fuel*, 404:136160, 2024.

[11] B. Zhao, P. Yang, N. Zhang, et al. Sulfonated hierarchical zsm-5 zeolite monolith as solid acid catalyst for esterification of oleic acid. *Chemical Communications*, 60:13356–13359, 2024.

[12] Q. Y. Zhang, X. Y. Hong, J. Lei, et al. Environmentally-friendly preparation of sr(ii)-bdc supported heteropolyacid as a stable and highly efficient catalyst for esterification reaction. *Journal of Saudi Chemical Society*, 28:101832, 2024.

[13] O. Ilgen and F. Baytas. Kinetic and parametric studies on oleic acid esterification catalyzed by pumice (t.s.i.). *Chemical Engineering & Technology*, 47:e202400141, 2024.

[14] M. Cao, M. Lu, H. Yin, et al. Effect of hemicellulose extraction pre-treatment on sulfonated corncob biochar for catalytic biodiesel production. *Journal of Environmental Chemical Engineering*, 11: 100058, 2023.

[15] Y. Zhao and G. Li. Construction of $h_3pmo_{12}o_{40}$@eb-cof for biodiesel preparation by heterogeneous analytical esterification of oleic acid and rapeseed oil. *Journal of Inorganic and Organometallic Polymers and Materials*, 35:46–57, 2025.

[16] Q. Y. Zhang, D. D. Lei, Q. Z. Luo, et al. Mof-derived zirconia-supported keggin heteropoly acid nanoporous hybrids as a reusable catalyst for methyl oleate production. *RSC Advances*, 11: 8117–8123, 2021.

[17] A. M. Rezadoost, S. Sadjadi, and A. Heydari. 3d-printed metal-organic framework encapsulated keggin heteropolyacid for catalytic purpose. *Journal of Molecular Structure*, 1305:137808, 2024.

[18] A. Bhuyan and M. Ahmaruzzaman. One-pot fabrication of a stable pom/mil-101(fe) hybrid catalyst supported on a chitosan biopolymer matrix: A study on biodiesel production through rsm optimization, experimental studies, and mechanistic insight. *Renewable Energy*, 241:123560, 2025.

[19] Y. Yu, Y. Li, Y. Fang, et al. Recent advances of ammonia synthesis under ambient conditions over metal-organic framework based electrocatalysts. *Applied Catalysis B: Environmental*, 340:123161, 2024.

[20] Y. Liu, Y. Xiong, C. Jin, et al. Cu-ce mof-based heterojunction catalysts for the electrooxidation of 5-hydroxymethylfurfural. *Industrial Crops and Products*, 226:120714, 2025.

[21] Y. Zhu, X. Nie, and X. Liu. Preparation of fe/co bimetallic mof photofenton catalysts and their performance in degrading tetracycline hydrochloride pollutants efficiently under visible light. *Journal of Alloys and Compounds*, 1010:176967, 2025.

[22] R. Pavadai, P. Anwarisan, S. Prahu, et al. An innovative hierarchical flower-like nimo-mof as a bifunctional electrocatalyst for enhanced orr and her performance. *Materials Chemistry and Physics*, 345:131245, 2025.

[23] Q. Zhang, Y. Wu, X. Hong, et al. Different ligand functionalized bimetallic (zr/ce)uio-66 as a support for immobilization of phosphotungstic acid with enhanced activity for the esterification of fatty acids. *Sustainable Chemistry and Pharmacy*, 37:101344, 2024.

[24] Y. Huang, J. Wang, S. Ma, et al. Enhanced adsorption-oxidation performance of pmo_{12} immobilized onto porous mcm-41 derived from rice husk for h_2s at room temperature. *Fuel*, 333:126448, 2023.

[25] L. Mi, B. Chen, X. Xu, et al. Room temperature synthesized layered cau-17 mofs for highly active and selective electrocatalytic co_2 reduction to formate. *Journal of Alloys and Compounds*, 978: 173516, 2024.

[26] X. Zang, H. Sun, W. Wang, et al. Plasma-catalytic removal of toluene over bimetallic m/mo-btc catalysts in dielectric barrier discharge reactor. *Separation and Purification Technology*, 331: 125567, 2024.